Journal of Optoelectronics and Advanced Materials Vol. 7, No. 2, April 2005, p. 951 - 954

STUDY OF a-Si:H TAIL STATE DISTRIBUTIONS THROUGH ANALYTICAL MULTIPLE-TRAPPING MODELLING[&]

E. V. Emelianova[*], M. Brinza, V. I. Arkhipov[a], G. J. Adriaenssens

University of Leuven, Halfgeleiderfysica, Celestijnenlaan 200D, B-3001 Leuven, Belgium
[a]IMEC, Kapeldreef 75, B-3001 Leuven, Belgium

By fitting analytical expressions for the multiple-trapping carrier transport process to experimentally measured transient photocurrent traces from hydrogenated amorphous silicon (a-Si:H) samples, it becomes possible to deduce realistic tail state distributions from the data. For instance: A strong Gaussian component to the valence band distribution of tail states is able to account for the field-independence of the hole drift mobility in a-Si:H samples prepared under high-deposition-rate conditions in an expanding thermal plasma.

(Received February 9, 2005; accepted March 23, 2005)

Keywords: Hydrogenated amorphous silicon, Tail states, Analytical modelling

1. Introduction

While an exponential distribution of tail states has been widely accepted as offering a good description of the density of localised states (DOS) near the mobility edge of both valence and conduction bands in hydrogenated amorphous silicon (a-Si:H) [1], discrepancies between experimental data and the theoretical model have always been observed … as well as largely ignored. Such discrepancies include the difference in dispersion parameters resolved from pre- and post-transit currents in time-of-flight (TOF) transient photocurrent experiments as opposed to the single one predicted for the exponential DOS, or the observation in some samples of field-independent drift mobilities together with dispersive transport characteristics.

Traditionally [2], the multiple-trapping transport equations that are used to describe the TOF signals are solved for the case of an exponential distribution $g(E) = g(0)\exp(-E/E_0)$, where E is the energy of a localised state and E_0 the characteristic width of the distribution, to yield current-time dependencies of $I(t) \propto t^{-(1-\alpha)}$ for $t<t_T$ and $I(t) \propto t^{-(1+\alpha)}$ for $t>t_T$. The transit time, t_T, that separates the two power laws signals the arrival, at the back electrode of the TOF sample, of the mean of the carrier packet that was generated at $t = 0$ at the front electrode. Experimentally, t_T can be resolved from the change of slope in the current traces as may be obvious from the curves in Fig. 1a. The parameter α in the power laws is related to the width of the exponential $g(E)$ through $\alpha = kT/E_0$. The pre-transit slope is, therefore, frequently used to estimate the exponential width E_0. A further relationship that can be used for that purpose is the electric field dependence of the carrier drift mobility $\mu_d = L/t_T F$, with L the sample thickness and F the applied field. For an exponential DOS, $\mu_d \propto (L/F)^{1-1/\alpha}$ will be observed and $E_0 = kT/\alpha$ can be extracted.

However, the practice outlined above does not always lead to consistent results. The examples shown in Fig. 1 illustrate the point. Figs. 1a and 1b show hole current transients and drift mobility field dependences from samples that exhibits the behaviour expected for an exponential valence band DOS. The remaining Figs. 1c and 1d relate to different samples where the current

[*] Corresponding author: zhenia.emelianova@fys.kuleuven.ac.be

[&]Paper presented at the International School on Condensed Matter Physics, Varna, Bulgaria, September 2004

traces still show the decaying power law that allows the extraction of the dispersion parameter α, but the drift mobility turns out to be field-independent at all measured temperatures. Since only a constant $\alpha = 1$, rather than any $\alpha = kT/E_0$, satisfies this latter observation, an exponential DOS cannot explain those data. A more fundamental approach to the problem is clearly required.

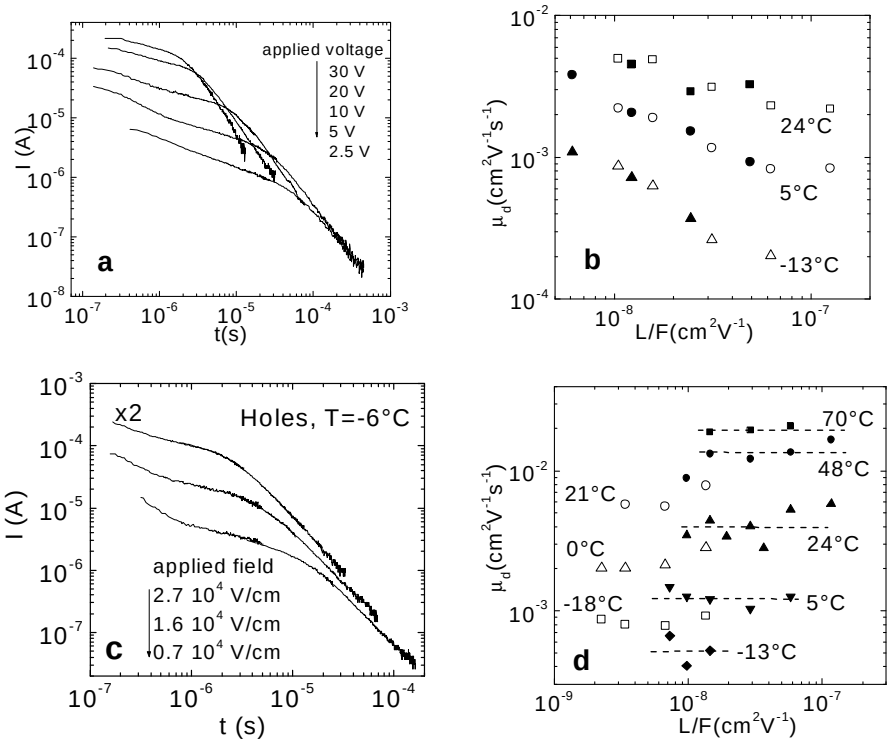

Fig. 1. (a) and (c) Examples of a-Si:H TOF hole current transients, showing the pre- and post-transit power laws; (b) and (d) The hole drift mobility calculated from transients such as those in (a), respectively (c). The two kinds of symbols correspond in (b) to two samples deposited in identical conditions but having different thickness, and in (d) to two samples deposited in slightly different conditions. In (d) lines of constant mobility are added as guide to the eye.

2. Analytical multiple-trapping expressions for TOF transients

Experimental observation of dispersive current transients together with the drift mobility independent of the (thickness/field) ratio indicates that transition from the non-equilibrium (dispersive) to equilibrium (Gaussian) transport regime occurs at times close to carrier-packet transit time. This transition is caused by thermal equilibration of most charge carriers within the DOS distribution. It is important to note that, at low carrier densities typical for TOF measurements, carrier equilibration is possible only if the DOS function decreases with energy steeper than an exponential function [3]. Therefore, current transients, which combine characteristics of both dispersive and equilibrium transport, cannot be analysed in terms of the exponential DOS model.

The underlying physical mechanism is easy to understand. At low carrier density, the equilibrium energy distribution of localized carriers, $\rho_{eq}(E)$, is given by the product of the DOS and Boltzmann functions as

$$\rho_{eq}(E) \sim g(E)\exp(E/kT) \ . \tag{1}$$

Equation (1) carries two important messages: (i) since the total carrier density must be finite the integral of $\rho_{eq}(E)$ must converge at large energies independent of the temperature, which is possible if the function $g(E)$ decreases with energy steeper than an exponential, and (ii) most equilibrated

carriers must occupy states whose energies are close to the maximum of the product. $g(E)\exp(E/kT)$. Note that, under the dispersive transport conditions, most carriers are temporarily localized in the states with energies around the demarcation level $E_d(t)$. Therefore, it is straightforward to conclude that most carriers are equilibrated when the demarcation level has crossed the maximum of the equilibrium carrier distribution.

For a Gaussian DOS distribution $g(E) = (2/\pi)^{1/2}(N_t/\sigma)\exp(-E^2/2\sigma^2)$ of width σ, the equilibrium carrier distribution reaches the maximum at the energy $E_m = \sigma^2/kT$. Concomitantly, the equilibration time t_{eq} , calculated from the condition $E_d(t) = E_m$, is given by

$$t_{eq} = \nu^{-1} \exp\left[\sigma^2/(kT)^2\right] . \tag{2}$$

At times close to or larger than the equilibration time, the carrier packet mean velocity levels off and the carrier drift mobility calculated via the transit time t_T as $\mu_d = L/Ft_T$ becomes independent of the field and sample thickness. However, not all carriers are yet equilibrated at t_{eq} notably those which occupy localized states below E_m. Since these carriers are responsible for the emission-controlled post-transit current its shape remains dispersive. The pre-transit current at times shorter than t_{eq} is also controlled by a non-equilibrium carrier energy distribution and, therefore, it decreases with time. This is how an equilibrium drift mobility can co-exist with a dispersive shape of current transients. As shown in Fig. 2(a,b), the Boltzmann equilibrium cannot be established in materials with an exponential DOS function which leads to permanently dispersive shape of the carrier packet in sample fabricated from such materials. The process of carrier thermalisation that leads to an equilibration within a Gaussian DOS distribution is illustrated in Fig. 3, together with its effect on the spatial distribution of carriers in the sample.

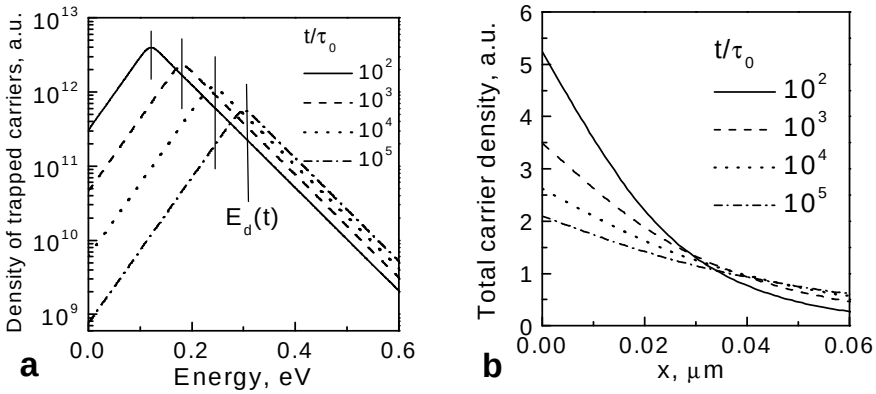

Fig. 2. Evolution in time of trapped (a) and total (b) carrier densities in a material with exponential DOS.

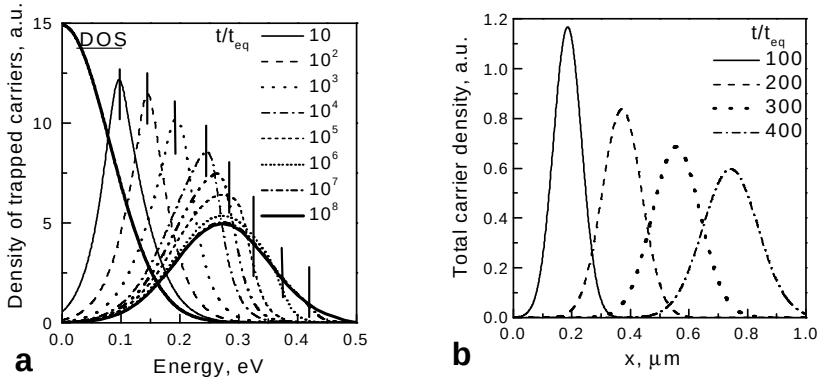

Fig. 3. Evolution in time of trapped (a) and total (b) carrier densities in the material with Gaussian DOS.

In order to examine TOF transients as shown in Fig. 1 with a combined DOS

$$g(E) = \frac{N_{tE}}{E_0}\exp\left(\frac{-E}{E_0}\right) + \left(\frac{2}{\pi}\right)^{1/2}\frac{N_{tG}}{\sigma}\exp\left(\frac{-(E-E_G)^2}{2\sigma^2}\right), \tag{3}$$

we have used the detailed multiple-trapping analysis of Arkhipov and Rudenko [4]. The general expression for the transient current can be written as

$$\begin{aligned} j(t) &= e\mu(t)(\sigma_0/L)F - e(\sigma_0/L)\lambda(t)\langle x\rangle(t), \quad t \le t^*, \\ j(t) &= e\mu(t)(\sigma_0/L)F\{1-\exp(-\Lambda(t)+\Lambda[t_0(t)])\} - e(\sigma_0/L)\lambda(t) \\ &\quad \{\langle x\rangle(t) - \exp(-\Lambda(t)+\Lambda[t_0(t)])\langle x\rangle[t_0(t)]\}, \quad t > t^*, \end{aligned} \tag{4}$$

where the various functions and parameters such as t^* are defined by the set

$$\begin{aligned} &x_0(t) - x_0[t_0(t)] = L; \qquad x_0(t^*) = L; \\ &\Lambda(t) = \int_0^t dt'\lambda(t'); \qquad \lambda(t) = \theta(t)[1+\theta(t)]^{-1}[1/\tau(t)]; \\ &1/\theta(t) = \int_0^{E_d(t)} dE[g(E)/N_C]\exp(E/kT); \quad 1/\tau(t) = (1/\tau_0)\int_{E_d(t)}^{\infty} dE\, g(E)/N_t; \\ &E_d = kT\ln(\nu t); \qquad \mu(t) = \theta(t)[1+\theta(t)]^{-1}\mu_0; \\ &x_0(t) = \int_0^t dt'\mu(t')E; \qquad \langle x\rangle(t) = \int_0^t dt'\mu(t')E\exp\{-[\Lambda(t)-\Lambda(t')]\}. \end{aligned} \tag{5}$$

In the above, σ_0 is the photoinduced carrier density, T is the temperature, k the Boltzmann constant, ν the attempt-to-escape frequency, N_t the total density of localized states, τ_0 the free-carrier lifetime, N_c the density of states at the mobility edge, μ_0 the free-carrier mobility. The equations are able to describe both dispersive and equilibrium transport regimes as well as transition from the former to the latter.

Using the above set of equations (3)-(5) to fit the TOF transient currents of the sample that resulted in the field-dependent mobilities shown by the open symbols in Fig. 1b, we obtain a DOS defined by the parameters $N_{tE} = 10^{21}$ cm^{-3}, $E_0 = 0.04$ eV for the exponential part and $N_{tG} = 2.5 \times 10^{20}$ cm^{-3}, $E_G = 0.02$ eV, $\sigma = 0.09$ eV for the Gaussian function. In other words, the exponential component dominates the tail states of this sample. The same exercise for one of the a-Si:H films that gave the field-independent mobilities seen in Fig. 1d results in the values $N_{tE} = 6 \times 10^{18}$ cm^{-3}, $E_0 = 0.04$ eV, $N_{tG} = 2.5 \times 10^{19}$ cm^{-3}, $\sigma = 0.087$ eV, and $E_G = 0.06$ eV. In this case, therefore, the Gaussian component dominates, as expected on the basis of the field independence of the mobility. Further examples and more details concerning the procedure may be found in Refs. [5-7].

References

[1] R. A. Street, Hydrogenated amorphous silicon, Cambridge University Press, Cambridge U.K. (1991).
[2] T. Tiedje, The Physics of Hydrogenated Amorphous Silicon II, Eds. J. D. Joannopoulos, G. Lucovsky, Springer-Verlag, Berlin, 1984, p. 261.
[3] A. I. Rudenko, V. I. Arkhipov, Philos. Mag. B **45**, 177 (1982).
[4] V. I. Arkhipov, A. I. Rudenko, Philos. Mag. B **45**, 189 (1982).
[5] M. Brinza, E. V. Emelianova, A. Stesmans, G. J. Adriaenssens, Mater. Res. Soc. Symp. Proc. **808**, 85 (2004).
[6] M. Brinza, E. V. Emelianova, Proceedings CAS 2004, IEEE Publications, 2004, p. 73.
[7] M. Brinza, G. J. Adriaenssens, J. Optoelectron. Adv. Mater. **7**(1), 73 (2005).